DOI 10.1002/mnfr.201700128 *Mol. Nutr. Food Res. 61, 9,* 2017, 1700128

RESEARCH ARTICLE

Muscle metabolic alterations induced by genetic ablation of 4E-BP1 and 4E-BP2 in response to diet-induced obesity

Olivier Le Bacquer[1], Kristell Combe[1], Christophe Montaurier[1], Jérôme Salles[1], Christophe Giraudet[1], Véronique Patrac[1], Carla Domingues-Faria[1], Christelle Guillet[1], Katie Louche[2], Yves Boirie[1,3], Nahum Sonenberg[4], Cédric Moro[2] and Stéphane Walrand[1]

[1] Université Clermont Auvergne, INRA, Clermont-Ferrand, France
[2] INSERM UMR1048, Institut des Maladies Cardiovasculaires et Métaboliques, Université Paul Sabatier, Toulouse, France
[3] CHU Clermont-Ferrand, Service Nutrition Clinique, Clermont Ferrand, France
[4] Department of Biochemistry, McGill University, Montreal, QC, Canada

Received: February 6, 2017
Revised: April 7, 2017
Accepted: April 18, 2017

Scope: In recent years, several studies reported the role of eIF4E-binding proteins (4E-BPs) on the development of diet-induced obesity and insulin resistance. Our aim was to investigate the effect of 4E-BP protein deletion on lipid accumulation and metabolism in skeletal muscle in response to a high-fat diet induced obesity in 4E-BP1/2 DKO mice.

Methods and results: Diet-induced obesity engendered increased ectopic accumulation of lipotoxic species in skeletal muscle of 4E-BP1 and 4E-BP2 double knockout mice (4E-BP1/2 DKO), namely diacylglycerols and ceramides. Increased lipid accumulation was associated with alterations in the expression of genes involved in fatty acid transport (FATP, CD36), diacylglycerol/triacylglycerol biosynthesis (GPAT1, AGPAT1, DGAT1), and β-oxidation (CPT1b, MCAD). Diet-induced obesity resulted in increased lean mass and muscle in 4E-BP1/2 DKO mice despite the development of a more severe systemic insulin resistance. Since increased expression of genes of several proteolytic systems (MuRF1, atrogin/MAFbx, and cathepsin-L) in 4EBP1/2 DKO skeletal muscle was reported, the increase of skeletal muscle mass in 4E-BP1/2 DKO mice suggests that ablation of 4E-BPs compensate with activation of muscle anabolism.

Conclusions: These findings indicate that 4E-BP proteins may prevent excess lipid accumulation in skeletal muscle and suggest that 4E-BPs are key regulators of muscle homeostasis regardless of insulin sensitivity.

Keywords:
ATGL / Lipid accumulation / Lipotoxicity / mTOR / Protein homeostasis

Additional supporting information may be found in the online version of this article at the publisher's web-site

1 Introduction

The mammalian target of rapamycin (mTOR) is a highly conserved serine/threonine kinase protein and a central sensor linking nutrient availability to cell growth and proliferation as well as numerous cellular processes in skeletal muscle [1]. mTOR forms two distinct functional complexes, mTOR complex 1 (mTORC1) and mTOR complex 2 (mTORC2). Once activated by nutrients or growth factors, mTORC1 phosphorylates downstream targets such as the S6-protein kinase (S6K) and the eukaryotic translation initiation factor 4E-binding proteins (4E-BPs) [2, 3]. In mammals, the 4E-BP family consists of three proteins, 4E-BP1, 4E-BP2, and 4E-BP3, which exhibit tissue-specific expression [4, 5]. The 4E-BPs compete with eIF4G for a shared binding site on eIF4E as the binding of 4E-BPs and eIF4G to eIF4E are mutually exclusive [6]. Binding of 4E-BP to eIF4E is regulated through phosphorylation: whereas hypophosphorylated forms strongly interact with eIF4E, hyperphosphorylation of 4E-BPs dramatically weakens this interaction [7]. In response to growth factors, or

Correspondence: Olivier Le Bacquer
E-mail: olivier.le-bacquer@inra.fr

Abbreviations: **4E-BP**, eIF4E-binding protein; **ATGL**, adipose triglyceride lipase; **DAG**, diacylglycerol; **HFD**, high-fat diet; **mTOR**, mammalian target of rapamycin; **TAG**, triacylglycerol; **T2D**, type II diabetes

nutrients, the mTORC1 sequential phosphorylation of 4E-BP proteins leads to their dissociation from eIF4E that results in increased cap-dependent translation initiation [6, 8, 9].

mTOR plays an important role in controlling the metabolic activity of organs such as skeletal muscle, adipose tissue, and liver to regulate whole-body energy homeostasis. mTOR chronic hyperactivation has been documented in peripheral tissues of obese humans and rodents and is associated with the development of insulin resistance [1, 10–13]. Conversely, nutritional interventions [14,15], pharmacological treatments [16,17], or genetic modifications of the mTOR pathway [13,18] counteract the negative effects of mTOR hyperactivity in obese mice. However, the key downstream targets of mTOR and their respective importance in controlling lipid homeostasis and ectopic accumulation in skeletal muscle are poorly understood.

In mammals, only few studies addressed the specific role of 4E-BPs in the control of glucose homeostasis and energy metabolism. 4E-BP proteins link mTORC1 activity and metabolism by regulating insulin sensitivity and adipogenesis [12, 19]. Indeed, we previously reported that mice lacking both 4E-BP1 and 4E-BP2 were more sensitive to diet-induced obesity and insulin resistance [12], a phenotype which is in agreement with the observation that protein level of 4E-BP1 is reduced in tissues of high-fat diet (HFD) fed mice [20]. In contrast, enhanced 4E-BP1 activity in mouse protects against age- and diet-induced insulin resistance and metabolic rate decline [20, 21]. Muscle-specific transgenic overexpression of a constitutively active form of 4E-BP1 in mice results in skeletal muscle fiber atrophy and attenuates physical performance. [21]. Also, we previously demonstrated that insulin resistance and impairment in muscle protein anabolism in response to diet-induced obesity was associated with intramuscular ectopic lipid accumulation [22], and it is largely documented that fat infiltration in muscle results in metabolic dysfunction leading to lipotoxicity and insulin resistance [22–24].

Notwithstanding the central role of 4E-BP proteins in the development of insulin resistance, adipogenesis, and obesity, it is unclear whether the previously documented increased adiposity in 4E-BP1/2 DKO mice protects skeletal muscle from lipid ectopic accumulation in the context of obesity. In the present study, 4E-BP1 and 4E-BP2 double knockout (DKO) mice were fed a HFD to examine the contribution of these proteins in the accumulation of lipids in skeletal muscle and examine how skeletal muscle lipid metabolism was altered.

2 Materials and methods

2.1 Chemicals

Insulin, L-leucine, DMEM containing 4.5 g/L glucose, anti-total p38 antibody, protease-inhibitor cocktail, puromycin, and primers were purchased from Sigma-Aldrich (Saint-Quentin-Fallavier, France). L-leucine-free DMEM was prepared by BioWest (Nuaillé, France). Fetal bovine and heat-inactivated horse sera, trypsin-EDTA, PBS, penicillin/streptomycin were obtained from PAA (Pasching, Austria). Primary antibodies were obtained from the following sources: anti-phospho p70 S6 kinase (Thr 389, #9205), anti-total p70 S6 kinase (#9202), anti-ATGL (#2138; where ATGL is adipose triglyceride lipase) (Cell Signaling Technology, Ozyme distributor, Saint-Quentin-en-Yvelines, France), anti-PLIN5 (#GP44), Progen, Heidelberg, Germany), mouse anti-puromycin mAb (clone 12D10) is described in [25]. Horseradish peroxidase conjugated secondary antibodies were purchased from DAKO (Trappes, France). SuperScript® III reverse transcriptase, random hexamer, and oligo dT primers were from Invitrogen (Life Technologies, Saint-Aubin, France). Tri-Reagent was purchased from Euromedex (Mundolsheim, France). Rotor-Gene SYBR Green PCR master mix was purchased from Qiagen (Courtaboeuf, France).

2.2 Animals and experimental design

Congenic BALB/c *Eif4ebp1*$^{-/-}$ *and Eif4ebp2*$^{-/-}$ mice (4E-BP1/2 DKO), previously described [12] were provided by Dr. Nahum Sonenberg (McGill University, Montréal, Canada). Only male mice were used in this study. Mice were individually housed in plastic cages and maintained at 21–23°C with a 12-h dark, 12-h light schedule and given free access to water and food. Twelve-week-old mice were fed either a control normal chow diet (D12450B; 20% protein, 70% carbohydrate, and 10% fat) or a HFD (D12492; 20% protein, 20% carbohydrate, and 60% fat) for 22 weeks (Research Diets, Inc.). The complete formulation of the diets is described in Supporting Information Table 2). Euthanasia was performed at 10 A.M. after an overnight fasting where mice had access to water. Genotype of each mouse was controlled by PCR at birth and at the end of the experiment. All breeding and experimental protocols were reviewed and approved by the local ethics committee for animal experimentation (CREFA Auvergne, agreement #00782.01) and adhered to the National Research Council's guideline for the care and use of laboratory animals.

2.3 Metabolic studies

Body weight and food intake were recorded weekly throughout the experimental protocol. Insulin and glucose tolerance tests were performed at the end of the diet. These tests were performed on mice after a 6 h fasting period. Insulin (1.2 mU/g) or glucose (2 mg/g) was intraperitoneally injected into mice ($n = 8$ for each group). Whole blood glucose concentration was measured in blood collected from the tail vein at the indicated time points, using an Accu-Check Advantage glucometer (Roche). Overnight fasting insulin level was measured by ELISA (EuroBio, Courtaboeuf, France). Plasma levels of fasting glucose, triglycerides, nonesterified fatty acids

(NEFA) and cholesterol were determined using a Konelab 20 analyzer (Thermo-Electron Corporation).

2.4 Indirect calorimetric studies

Energy expenditure, volunteer home cage activity, and food and water intake were measured by using a four-cage TSE System Pheno-Master/LabMaster (Bad Homburg, Germany). Spontaneous activity was measured using a three dimensions meshing of light beams.

2.5 Statistical analysis

Data are expressed as mean ± SEM. Differences between groups were analyzed with two-way ANOVA to test the effect of genotype and diet. Bonferroni post-tests were used to compare replicate means by row. A p value of 0.05 was considered statistically significant.

The complete methods for RNA extraction and quantitative real-time PCR, cell culture and western blot, determination of triacylglycerol (TAG), diacylglycerol (DAG), and ceramide content in muscle tissue and ATGL activity assay are described in Supporting Information.

3 Results

3.1 Loss of 4E-BP induces muscle lipid ectopic accumulation

To study the role of 4E-BP1 and 4E-BP2 proteins in skeletal muscle in the context of obesity, 12-week-old WT and 4E-BP1/2 DKO mice were fed a standard chow diet (CTL) or a HFD for 22 weeks. As previously described [12], 4E-BP1/2 DKO mice weighed significantly more than WT mice in both CTL and HFD conditions (Fig. 1A). The increase in body weight was associated with a slight increase in food intake in 4E-BP1/2 DKO mice in both CTL and HFD conditions (Fig. 1B) and reduced energy expenditure (Fig. 2B). 4E-BP1/2 DKO mice exhibited a similar glucose homeostasis to WT mice, including a normal insulin response and glucose clearance rate on CTL diet. HFD leads to a dysregulation of glucose homeostasis in both WT and 4E-BP1/2 DKO mice (Supporting Information Table 1). However, the HFD-induced insulin resistance and glucose intolerance was higher in 4E-BP1/2 DKO as compared to WT mice (Fig. 1C and D).

We next characterized the alterations associated with the increased insulin resistance in 4E-BP1/2 DKO muscle. Exposure of skeletal muscle to excessive lipids leads to accumulation of fatty acid derived metabolites such as TAG, DAG, ceramides, and sphingomyelins. It is widely accepted that ectopic accumulation of lipids is associated with insulin resistance [23, 26, 27]. Therefore, we measured the accumulation of these compounds in WT and 4E-BP1/2 DKO muscle in response to CTL or HFD. TAG muscle content was unaltered in 4E-BP1/2 DKO either on CTL or HFD as compared to WT (Fig. 2A). However, DAG content (Fig. 2B) was increased in muscle of 4E-BP1/2 DKO mice in CTL diet (1.98 ± 0.11 versus 1.46 ± 0.06 nmol/mg proteins, $p < 0.05$) and by HFD (14.33 ± 1.38 versus 9.24 ± 0.98 ng/mg proteins, $p < 0.01$). Ceramide and sphingomyelin levels were unchanged under CTL diet, but all increased by HFD in 4E-BP1/2 DKO muscle as compared to WT (Fig. 2C and D, $p < 0.01$). The increased DAG content and unaffected TAG content in 4E-BP1/2 DKO muscle prompt us to analyze the expression and activity of ATGL, which catalyzes the first step of TAG hydrolysis into DG [28]. mRNA expression of ATGL in skeletal muscle was increased in 4E-BP1/2 DKO muscle as revealed by two-way ANOVA (Fig. 3A, $p < 0.05$). However, ATGL protein expression (Fig. 3B and C) and activity (Fig. 3D) were unchanged in 4E-BP1/2 DKO muscle on HFD as compared to WT muscle. To further analyze the mechanisms responsible for the accumulation of lipotoxic compounds, we measured the mRNA levels of genes involved in fatty acid transport, DAG/TAG metabolism and fatty acid β-oxidation in skeletal muscle. LPL mRNA expression was unaffected by 4E-BP protein deletion, but the expression of FATP and CD36 mRNA (involved in the transport of fatty acids) was increased in 4EBP1/2 DKO muscle (Fig. 4A). It also impacted DAG/TAG homeostasis by increasing the mRNA expression of GPAT1 and AGPAT1, which catalyze the first two steps in DAG synthesis from glycerol-3-phosphate [29], and by increasing the mRNA expression of DGAT1, which catalyze the final step in mammalian TAG synthesis [30] (Fig. 4B). Last, genotype impacted β-oxidation by increasing the mRNA expression of CPT1B and MCAD (Fig. 4C). Altogether these data suggest that deletion of 4E-BP proteins results in alterations in lipid metabolism in muscle and increase lipid accumulation.

3.2 Loss of 4E-BPs induces gain of muscle mass

The analysis of body composition by echoMRI revealed that fat mass content was similar between WT and 4E-BP1/2 DKO at the end of the diet regimen in both CTL and HFD conditions (Fig. 1E). Lean mass content was higher in 4EBP1/2 DKO mice as compared to WT mice in CTL diet. Surprisingly, HFD induced a pronounced gain of lean mass in 4EBP1/2 DKO mice (Fig. 1F). Several tissues were collected at the end of the diet regimen. There was no difference in the weight for either adipose tissue (gonadal and subcutaneous) or liver between the WT and 4E-BP1/2 DKO mice regardless of the diet (Table 1). Analysis of the hindlimb reveals an increase in the weight of several muscles in 4E-BP1/2 DKO mice fed a CTL diet, notably soleus ($p < 0.05$) and plantaris muscles ($p < 0.05$). HFD leads to increased muscle mass in WT mice that was significantly more pronounced in 4E-BP1/2 DKO mice (Table 1). The locomotor activity was determined for WT and 4E-BP1/2 DKO mice during the light and dark cycle. During the light phase, we observed that the traveled

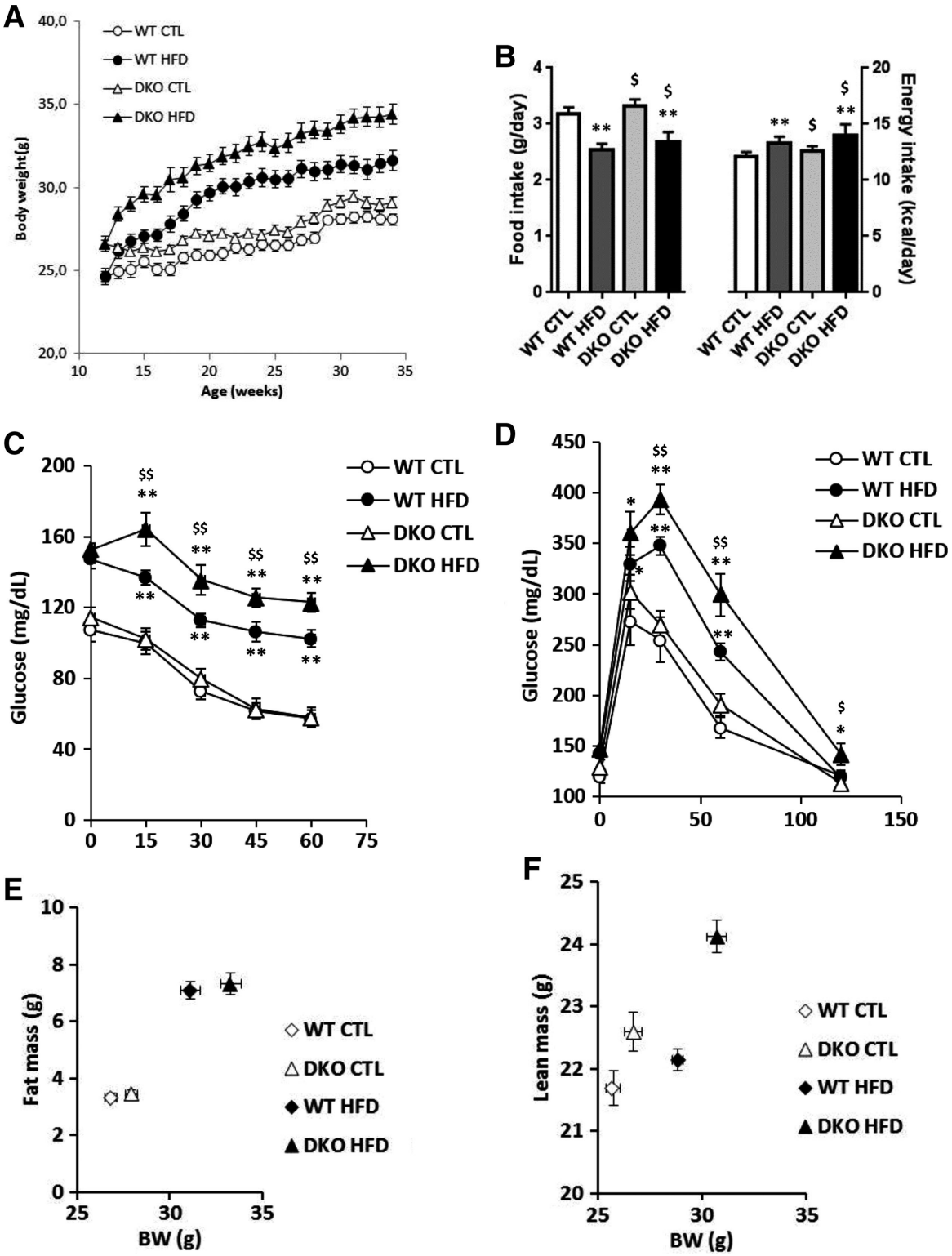

Figure 1. Loss of 4E-BP1 and 4E-BP2 leads to increased body weight and altered insulin sensitivity. (A) Body weight measurement in male mice ($n = 14$–18 per genotype). (B) Food consumption per day. (C) Insulin sensitivity was measured after intraperitoneal injection of insulin as described in Section 2 and expressed as area under the curve. (D) Glucose tolerance was measured after intraperitoneal injection of glucose as described in Section 2 and expressed as area under the curve. (E and F) measurement of fat (E) and lean mass (F) by echoMRI at the end of the diets. *p* values were assessed by two-way ANOVA. Bonferroni post-tests were used to compare replicate means by row. $^{*}p < 0.01$ versus CTL; $^{**}p < 0.01$ versus CTL; $^{\$}p < 0.05$ versus WT; $^{\$\$}p < 0.01$ versus WT.

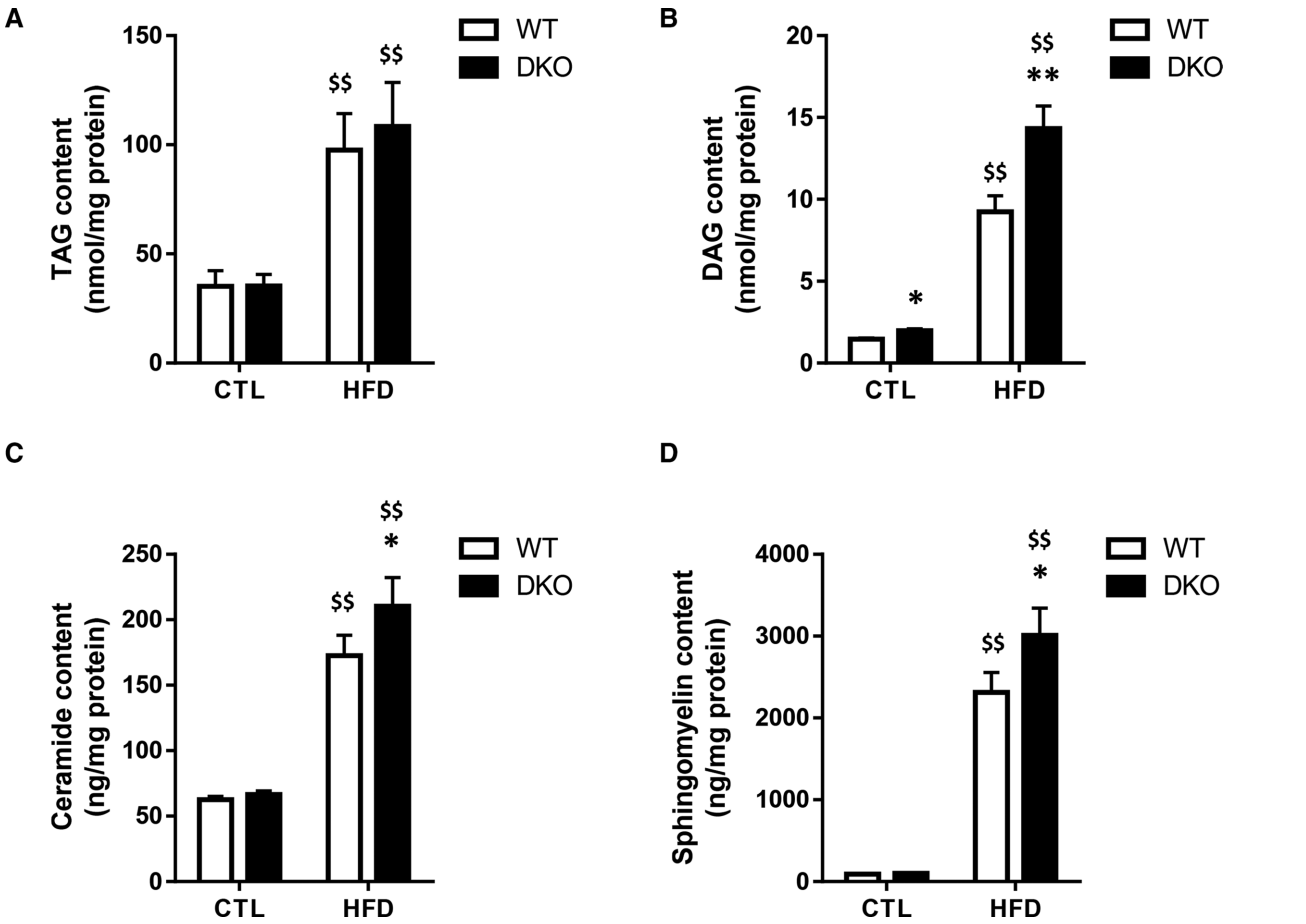

Figure 2. Indirect calorimetry and spontaneous locomotor activity in WT and 4E-BP1/2 DKO mice. (A) Energy expenditure in WT and 4E-BP1/2 DKO mice fed CTL or HFD ($n = 7$ per genotype). (B) Spontaneous locomotor activity in WT and 4E-BP1/2 DKO was measured using infrared sensor pairs arranged in strips for horizontal (left panel) and vertical (right panel) activity. (C) Representative data acquisition of the vertical activity of WT and 4E-BP1/2 DKO mice. p values were assessed by two-way ANOVA. Bonferroni post-tests were used to compare replicate means by row. *$p < 0.05$ versus WT; **$p < 0.01$ versus WT; $^{\$}p < 0.05$ versus CTL; $^{\$\$}p < 0.01$ versus CTL.

distance was reduced in WT mice fed a HFD as compared to CTL diet (Fig. 5B, left panel; $p < 0.05$). The traveled distance was similar in WT CTL diet as compared to 4E-BP1/2 DKO CTL diet and in WT HFD diet as compared to 4E-BP1/2 DKO HFD diet. Regardless of the diet, no difference in traveled distance was observed between WT and 4EBP1/2 DKO in the dark phase (Fig. 5B, left panel). However, we observed that 4E-BP1/2 DKO mice spent about twice more time in the vertical position as compared to WT mice in both CTL and HFD conditions (Fig. 5B, right panel and C). As expected, for each parameter, values were significantly higher in the dark phase than in the light phase ($p < 0.05$).

3.3 Loss of 4E-BPs alters protein homeostasis

Protein content was increased by ≈12% in 4E-BP1/2 DKO gastrocnemius on CTL diet (93.5 ± 2.3 versus 83.5 ± 2.6 μg protein/mg tissue, $p < 0.01$) (Fig. 6A). HFD induced an increase in muscle protein content in both WT and 4EBP1/2 DKO muscle, with protein content remaining ≈10% higher in 4E-BP1/2 DKO (100.0 ± 2.7 versus 90.7 ± 2.1, $p < 0.01$). The increased protein content in 4E-BP1/2 DKO muscle can result from a reduction in proteolysis, increased protein synthesis, or a combination of both. To understand whether proteolysis was modified by the deletion of 4E-BP1 and 4E-BP2 proteins, we measured mRNA levels of MuRF1, MAFbx/atrogin, and cathepsin-L in gastrocnemius. The two-way ANOVA analysis revealed a positive effect of genotype on the expression of MuRF1 ($p < 0.001$), MAFbx/Atrogin ($p < 0.01$), and cathepsin-L ($p < 0.01$) mRNA levels which were all increased in 4E-BP1/2 DKO muscle as compared to WT muscle under both CTL and HFD conditions (Fig. 6B). MuRF1 and cathepsin-L mRNA levels were not affected by HFD whereas MAFbx/atrogin was significantly reduced in HFD mice ($p < 0.05$).

Our study was not designed to measure protein synthesis in vivo. Therefore, to investigate whether protein synthesis

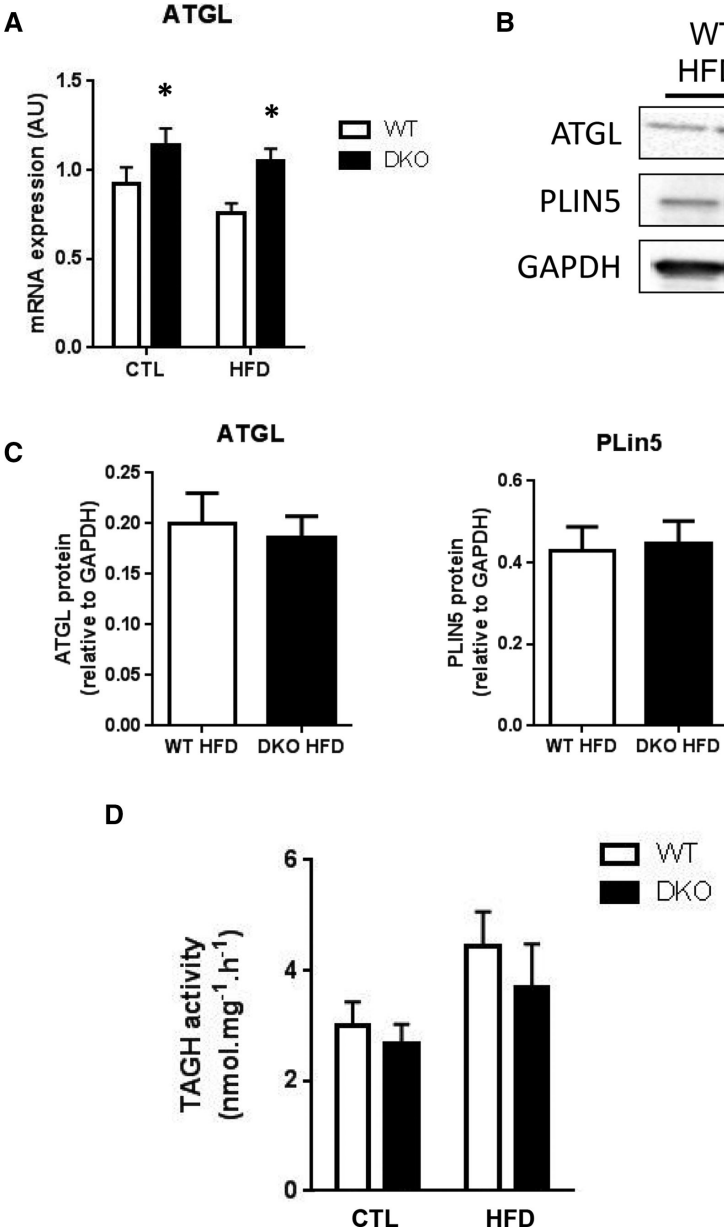

Figure 3. Loss of 4E-BP1 and 4E-BP2 alters protein homeostasis. (A) Protein content in gastrocnemius from WT and 4EBP1/2 DKO mice ($n = 10$–12 per genotype). (B) Real-time PCR quantification of proteolysis-related genes in gastrocnemius from WT and 4E-BP1/2 DKO mice ($n = 10$-12 per genotype). P values were assessed by 2-way ANOVA. Bonferroni post-tests were used to compare replicate means by row. $^{*}p < 0.05$ versus WT; $^{**}p < 0.01$ versus WT.

is altered by the deletion of 4E-BP proteins, primary MEFs from WT and 4E-BP1/2 DKO embryos were used to measure protein synthesis by using the SUnSET technique. As shown in Supporting Information Fig. 1 L-leucine/insulin or L-leucine/serum treatment induces a dose–response incorporation of puromycin into nascent proteins, an index of protein synthesis. The incorporation of puromycin was twice higher in unstimulated conditions in 4E-BP1/2 DKO MEFs (Supporting Information Fig. 1A–D, $p < 0.01$). Treatment of MEFs by increasing dose of insulin or increasing dose of serum leads to a dose–response stimulation of puromycin incorporation that was higher in 4E-BP1/2 DKO MEFs (Supporting Information Fig. 1A and B). For L-leucine/insulin stimulation, maximal incorporation of puromycine was achieved with a 10 nM insulin dose in DKO MEFs as compared to 100 nM for WT MEFs (Supporting Information Fig. 1B, $p < 0.01$). The amplitude of dose–response incorporation of puromycin with serum was similar between WT and DKO MEFs (Supporting Information Fig. 1D). Previous studies demonstrated that phosphorylation of S6K1 was elevated in tissues of mice lacking 4E-BP1 and 4E-BP2 [12, 31]. Therefore, phosphorylation state of S6K1 in primary MEFs was analyzed. Phosphorylation of S6K1 was dose dependently increased in 4E-BP1/2 DKO primary MEFs in response to L-leucine/insulin or L-leucine/serum treatment (Supporting Information Fig. 1A–D). Overall these data suggest that deletion of 4E-BP proteins resulted in modification of protein homeostasis.

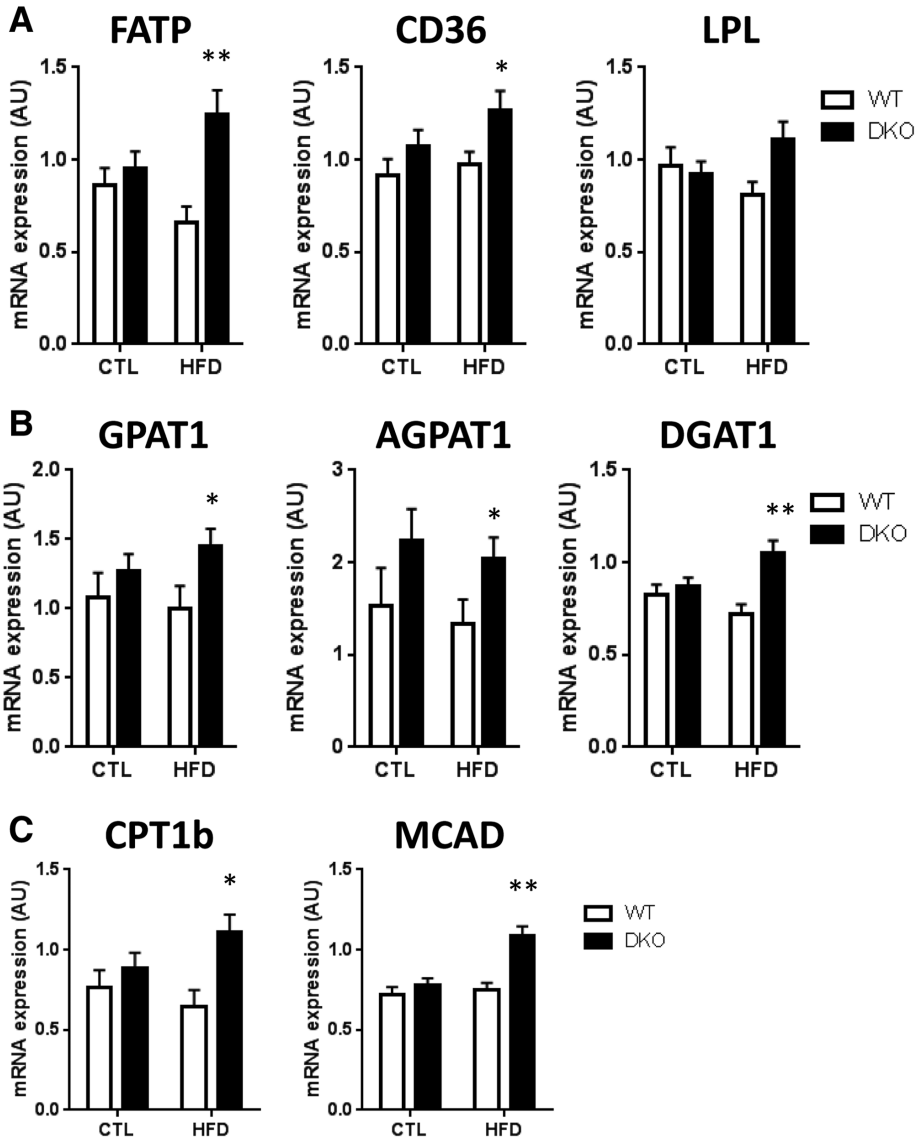

Figure 4. Loss of 4E-BP1 and 4E-BP2 promotes ectopic lipid accumulation in skeletal muscle. Total TAG (A), DAG (B), ceramide (C) and sphingomyelin contents (D) in tibialis of WT and 4EBP1/2 DKO mice under CTL or HFD (n = 10-12 per genotype). p values were assessed by two-way ANOVA. Bonferroni post-tests were used to compare replicate means by row. *$p < 0.05$ versus WT; **$p < 0.01$ versus WT.

Table 1. Hindlimb skeletal muscle and tissue weight in WT and 4EBP1/2 DKO mice

	WT		4E-BP1/2 DKO	
	CTL	HFD	CTL	HFD
Gastrocnemius (mg)	120.8 ± 1.6	125.4 ± 1.9	122.9 ± 1.2	130.7 ± 2.0 $^{\$\$}$
Soleus (mg)	8.3 ± 0.2	8.8 ± 0.2	9.3 ± 0.2 *	10.3 ± 0.3 $^{\$\$,**}$
Tibialis (mg)	48.7 ± 0.8	50.8 ± 0.9	50.0 ± 0.7	53.9 ± 0.9 $^{\$,*}$
EDL (mg)	11.2 ± 0.2	11.2 ± 0.4	12.0 ± 0.2	12.4 ± 0.1 *
Plantaris (mg)	15.1 ± 0.2	16.6 ± 0.3 $^{\$}$	17.1 ± 0.3**	17.6 ± 0.4
Quadriceps (mg)	213.7 ± 3.8	217.7 ± 3.8	220.4 ± 2.3	232.5 ± 4.3*
All muscles (mg)	418.1 ± 5.1	427.1 ± 7.1	431.7 ± 3.1	455.7 ± 9.5 $^{\$,*}$
GWAT (g)	537 ± 23	1005 ± 47 $^{\$\$}$	482 ± 35	970 ± 67 $^{\$\$}$
SWAT (g)	346 ± 19	629 ± 22 $^{\$\$}$	352 ± 28	702 ± 49 $^{\$\$}$
Liver (g)	1034 ± 14	1153 ± 15 $^{\$\$}$	1042 ± 17	1296 ± 39 $^{\$\$}$
Heart (mg)	151 ± 4	160 ± 3	167 ± 3	184 ± 7 *

Mice were 35-week-old. Results are expressed as mean ± SEM (n = 10–12). GWAT and SWAT: gonadal white adipose tissue, subcutaneous white adipose tissue. p values were assessed by two-way ANOVA. Bonferroni post-tests were used to compare replicate means by row. *$p < 0.05$, **$p < 0.01$ versus WT; $^{\$}p < 0.05$, $^{\$\$}p < 0.01$ versus CTL diet.

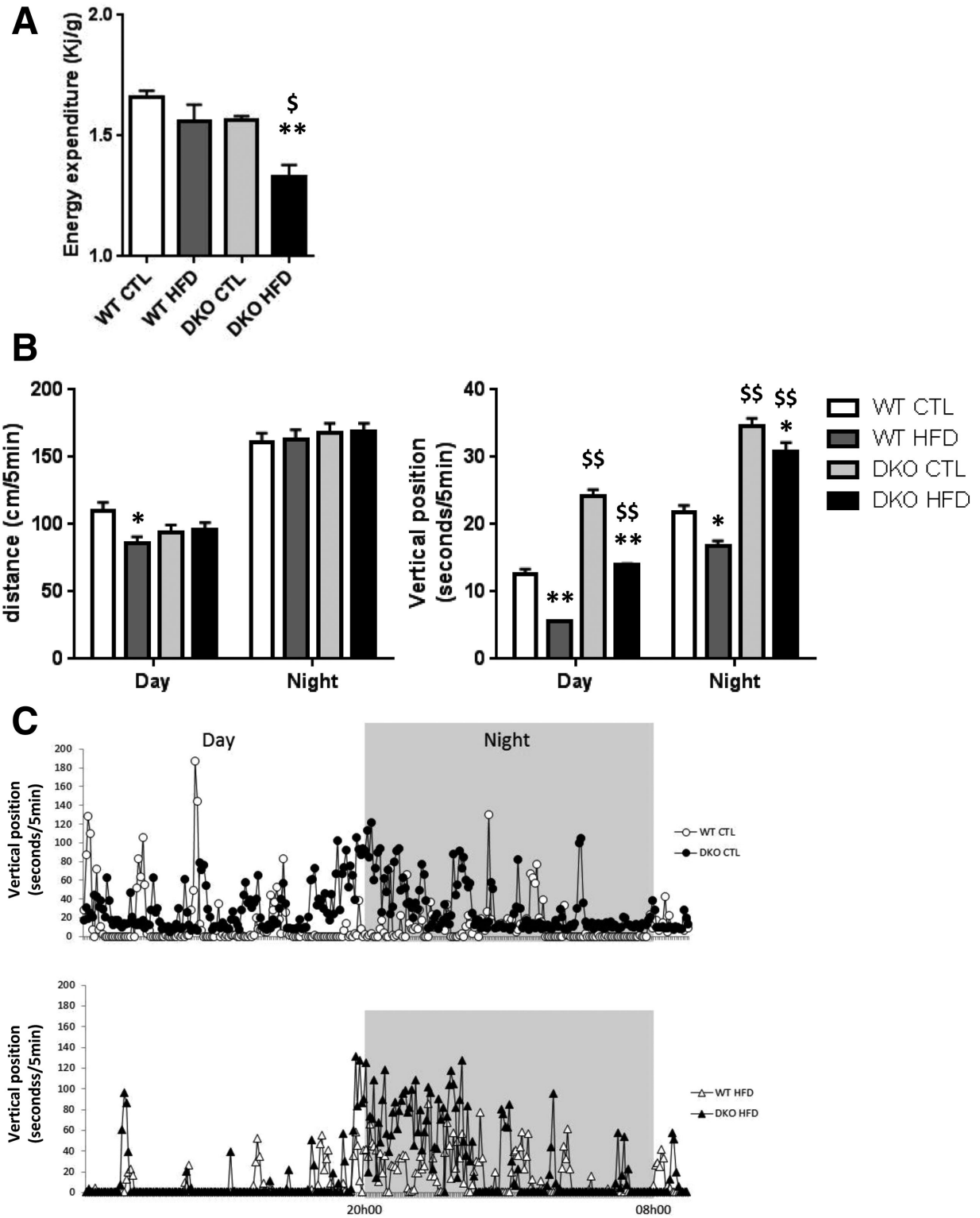

Figure 5. The increased accumulation of lipotoxic compounds in 4E-BP1/2 DKO muscle is independent of ATGL activity. (A) Real-time PCR quantification of ATGL mRNA expression in skeletal muscle from WT and 4EBP1/2 DKO mice fed a CTL or HFD ($n = 10$–12 per genotype). (B) Representative western blot analysis of ATGL and PLIN5 expression in skeletal muscle of WT and 4EBP1/2 DKO mice fed a HFD. (C) Quantification of ATGL (left panel) and PLIN5 (right panel) signal from (B). (D) Measurement of ATGL activity in skeletal muscle of WT and 4E-BP1/2 DKO mice fed a CTL or HFD. *p*-values were assessed by two-way ANOVA. Bonferroni post-tests were used to compare replicate means by row. $^{*}p < 0.05$ versus WT; $^{**}p < 0.01$ versus CTL; $^{\$}p < 0.05$ versus WT; $^{\$\$}p < 0.01$ versus WT.

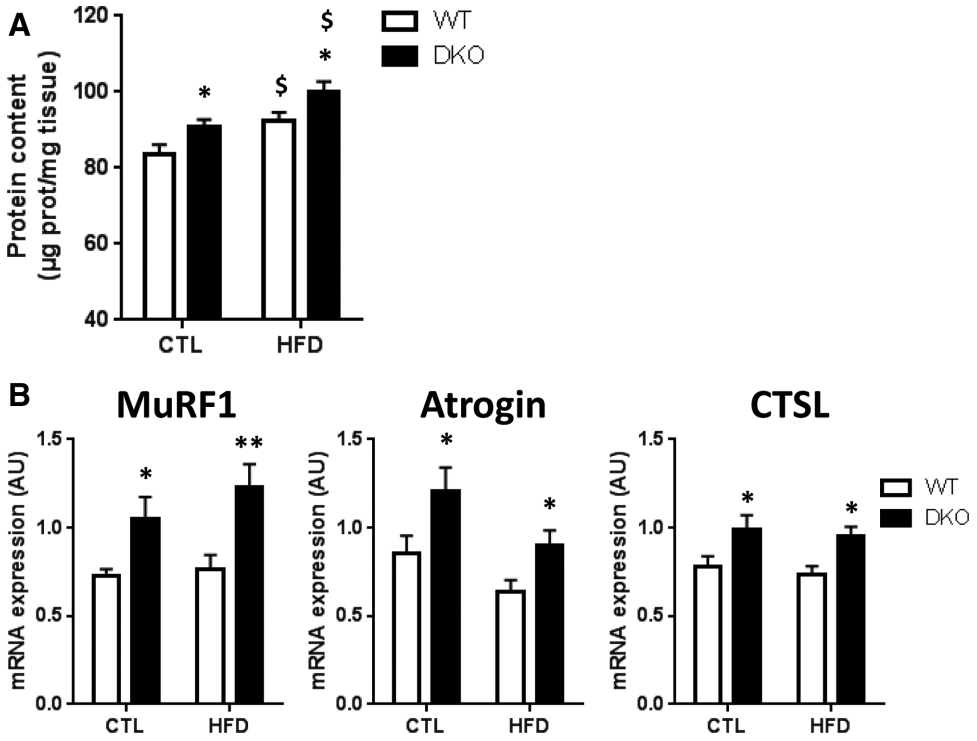

Figure 6. Loss of 4E-BP1 and 4E-BP2 alters lipid metabolism in skeletal muscle. (A) Real-time PCR quantification of fatty acid transport (A), DAG/triacyglyceride metabolism (B) and β-oxidation (C) related genes in skeletal muscle from WT and 4EBP1/2 DKO mice fed a CTL or HFD (n = 10–12 per genotype). p values were assessed by two-way ANOVA. Bonferroni post-tests were used to compare replicate means by row. $^{*}p < 0.05$ versus WT; $^{**}p < 0.01$ versus WT; $^{\$}p < 0.05$ versus CTL.

4 Discussion

In this study, we investigated the role of 4E-BP proteins in the changes of skeletal muscle metabolism in response to HFD-induced obesity. Under high-fat feeding, the genetic ablation of 4E-BP1 and 4E-BP2 promoted intramuscular accumulation of DAGs and ceramides, concomitantly with increased systemic insulin resistance. The accumulation of lipotoxic species was independent of changes in ATGL activity but associated with alterations in lipid metabolism gene expression (i.e., fatty acid transport, β-oxidation, triglyceride metabolism). Surprisingly, loss of 4E-BPs also increased muscle mass despite an increased whole body insulin resistance.

4.1 Deletion of 4EBP1 and 4EBP2 promotes skeletal muscle ectopic lipid accumulation in response to HFD

Muscle fat infiltration and concomitant lipotoxicity have deleterious effects on metabolic function and insulin resistance [22–24]. In agreement with the higher degree of insulin resistance in 4E-BP1/2 DKO mice (current results and [12]), we observed that loss of 4E-BPs promoted the accumulation of lipotoxic lipids species in skeletal muscle. The intramuscular accumulation of lipids is associated with increased mRNA expression of genes involved in TAG metabolism, fatty acid transport, and β-oxidation. The loss of 4E-BP proteins can be considered as a model of mTORC1 overactivity. In this regard, our results are in agreement with previous studies where increased or decreased expression of genes involved in fatty acid transport and oxidation was induced, respectively, by muscle-specific overactivation of mTORC1 by tuberous sclerosis complex 1 (TSC1) deletion (TSCmKO mouse) [32] and muscle-specific mTORC1 inactivation by raptor deletion (RAmKO mouse) [33]. TSCmKO mice are resistant to diet-induced obesity whereas 4E-BP1/2 DKO mice are more sensitive to diet-induced obesity [12]. Furthermore, RAmKO mice are also resistant to diet induced-obesity [33]. Altogether, this suggest that direct changes in mTORC1 complex core/activity and of its downstream targets (such as 4E-BP proteins) share common mechanisms that control the expression of lipid metabolism genes. In terms of diet-induced obesity, the 4E-BP1/2 DKO model might represent a less drastic model of mTORC1 overactivity as compared to the TSCmKO model since mTORC1 still needs growth factors, nutrients and insulin inputs to be activated whereas it is constitutively active when TSC1 has been ablated. Further study will be required to understand the alterations leading to different sensitivity to diet-induced obesity between these two mouse strains.

Surprisingly, although HFD results in an increased DAG accumulation in 4EBP1/2 DKO muscle, TAG content was similar in WT and 4E-BP1/2 DKO muscle. It is proposed that skeletal muscle lipid droplet dynamics may be an important determinant of lipotoxicity and insulin sensitivity [24]. Intramuscular lipid breakdown is operated by lipases. Among them, ATGL is highly specific for TAG and catalyzes the first step of their hydrolysis into DAG [24, 28]. Disturbance of lipase expressions and/or activities in skeletal muscle is

associated with lipotoxicity and insulin resistance [24]. Furthermore, a recent study demonstrated that 4E-BP proteins are able to control fat storage by regulating the expression of ATGL [34]. Despite these previous observations, ATGL protein level and activity were unaltered by the loss of 4E-BPs in mice fed with HFD. Hormone-sensitive lipase null mice display normal TAG but elevated DAG synthesis rate in muscle [35], a phenotype similar to the one we observed in the present study. However, a previous study demonstrated that hormone-sensitive lipase protein level and its phosphorylation on ser 595 (critical for its lipase activity) were unaltered in 4E-BP1/2 DKO adipose tissue, yet lipolysis was increased [12]. Altogether, these results suggest that the increased DAG content in 4E-BP1/2 DKO skeletal muscle is independent of lipid droplet dynamics and alteration of lipase activity.

4.2 Deletion of 4EBP1 and 4EBP2 increases skeletal muscle mass in response to HFD

In the present study, fat accumulation in response to HFD was similar between WT and 4EBP1/2 DKO mice. In a previous work, we observed that HFD was associated with increased fat accumulation in 4EBP1/2 DKO mice [12]. The age of the mice at the start of the diet (12 versus 8 weeks) as well as housing conditions (one mouse versus 2–3 mice/cage) was different between this study and the present one and we can only speculate that aging and/or housing may have interfere with some outcomes. Further studies would be required to fully answer this discrepancy. In the present study, whole body genetic ablation of 4E-BPs was associated with a slight increase in muscle mass that is amplified after high-fat feeding, despite the development of a systemic insulin resistance. This is surprising considering that insulin, together with amino acids, is an important regulator of protein anabolism [36, 37]. In addition to its deleterious effect on glucose uptake, the development of insulin resistance is reported to have detrimental effects on protein metabolism [38–40]. The effect of obesity on muscle mass is still debated. In general, obese subjects have larger lean body mass than nonobese subjects. The higher lean body mass could be in part related to skeletal muscle hypertrophy, which have to mechanically support the increased fat mass [41]. However, a lower muscle mass was reported in obese Zucker rats or leptin-deficient mice [42, 43], whereas muscle mass seems unchanged in diet-induced obesity animal models despite a higher fat deposition [44, 45]. In a rat model of diet-induced obesity, it was reported that changes in muscle mass are dependent on whether the animal is in the dynamic or in the static phase of obesity. Actually, an increased muscle mass was documented during weight gain, whereas chronically installed obesity was associated with a decrease in muscle mass [46]. Therefore, the onset of obesity and its exposure to a greater mechanical loads, which might have training-like effects on muscle mass, is likely a period of increased protein anabolism in skeletal muscle. We observed that 4E-BP1/2 DKO mice spend more time on vertical position as compared to WT mice. It is highly possible that deletion of 4E-BPs impacted the behavior of these mice. 4E-BPs are a family of three proteins (4E-BP1, 4E-BP2, and 4E-BP3) sharing the same role of translation initiation inhibitor but having a different tissue distribution [19]. To date, only 4E-BP2 has been observed in the brain and the 4E-BP2 knockout mice exhibited impaired spatial learning and memory [47, 48]. It is highly conceivable that 4E-BP1/2 DKO mice have the same alterations in memory that could explain the increased exploratory/vertical positioning behavior we observed. Therefore, the significantly higher weight and the increased vertical activity observed in 4E-BP1/2 DKO mice might result in such a training effect. However, the similar amplitude of body weight gain between WT and 4E-BP1/2 DKO in response to HFD suggests that other mechanisms are responsible for the increased muscle mass in 4E-BP1/2 DKO mice.

4.3 4E-BP proteins regulate protein homeostasis

How loss of 4E-BP proteins that leads to an increased systemic insulin resistance can be associated with an increased muscle mass gain in diet-induced obesity is questionable. Muscle-specific inactivation of mTOR leads to severe myopathy [49] and genetic deletion or knockdown of raptor or S6K1, which induces inactivation of mTORC1, are sufficient to prevent muscle growth and atrophy [50,51]. Similarly, transgenic mice overexpressing a constitutively active form of 4E-BP1 (which mimics inactivation of mTORC1) in skeletal muscle had a reduced lean body mass associated with a reduced muscle fiber size [21]. Conversely, short-term hyperactivation of mTORC1 by knockdown of TSC-induced muscle fiber hypertrophy and atrophy resistance upon denervation [50], and muscle overexpression of Rheb stimulates a PI3K/Akt independent activation of mTOR signaling sufficient for the induction of a hypertrophic response [52]. Altogether, these data suggest that muscle development can be driven by mTORC1 independently from upstream PI3K/Akt and insulin signaling.

To our knowledge, only two studies have previously approached the role of 4E-BPs in the control of protein synthesis. In the first study, Steiner et al. observed that basal skeletal muscle protein synthesis was unaltered in 4E-BP1/2 DKO mice, but protein synthesis in response to feeding was not measured [53]. In a second study, Signer et al. observed that deficiency in 4E-BP1 and 4E-BP2 significantly increased global protein synthesis in hematopoietic stem cells [54]. Muscle protein synthesis analysis was under the scope of our study. For technical reasons, we used primary MEFs to measure in vitro whether deletion of 4E-BP proteins might modify protein synthesis. We observed that it was increased in primary 4E-BP1/2 DKO MEFs in response to serum or insulin treatments. Additionally, increased S6K1 activity, a downstream target of mTORC1, has been documented in 4EBP1/2 DKO both in vivo and in vitro [12, 31] and is

observed in the present study. Overactivity of S6K1 is known to regulate a negative feedback on insulin signaling through inhibitory phosphorylation and degradation of IRS-1 [13, 55, 56] which reduces glucose uptake by the muscle and contributes to systemic insulin resistance. The in vitro observation that the induction of protein synthesis in primary 4E-BP1/2 DKO MEFS is associated with increased S6K1 phosphorylation could fill the gap between increased insulin resistance and protein synthesis: On one hand, the obesity-associated overactivity of mTORC1 through increased phosphorylation of S6K1 and negative feedback on IRS-1 mediates the development of systemic insulin resistance [12, 13]. On the other hand, loss of 4E-BP proteins (inhibitors of mRNA translation initiation) and S6K1 activity unleash brakes to promote protein synthesis. However, the results we obtained using primary MEFs need to be confirmed in skeletal muscle and will require further analysis.

We also observed an increased mRNA expression of several genes involved in proteolysis, which could be in disagreement with the stimulation of muscle protein accretion by loss of 4E-BP proteins. A recent study by Zhang et al. showed that mTORC1 activation not only was able to stimulate protein synthesis but also able to increase capacity for protein degradation [57]. The authors concluded that in addition to serving as quality control mechanism for newly translated proteins, the mTORC1-stimulated increase in proteasomal capacity could serve as an adaptive response to accompany increased protein synthesis downstream of mTORC1 by increasing cell amino acid availability. Therefore, the increased mRNA expression of MuRF1, MAFbx/atrogin and cathepsin-L could serve to maintain adequate pools of amino acids to sustain protein synthesis.

In summary, our results demonstrate that 4E-BP proteins are key determining factors in the development of systemic insulin resistance and that the deletion of these proteins is associated with increased ectopic accumulation of lipotoxic compounds and altered lipid metabolism in skeletal muscle in response to high-fat feeding. We also reveal that despite the development of systemic insulin resistance by HFD feeding, loss of 4E-BPs is able to induce an anabolic response in skeletal muscle. Our findings suggest that 4E-BPs are able to control a critical (yet unknown) mechanism where protein homeostasis is dissociated from its modulation by insulin. Therefore, 4E-BPs might represent an interesting pharmacological target to prevent muscle loss in situation of insulin resistance.

O.L.B., K.C., J.S., C.G., V.P. and C.G performed the animal experiments, cell culture, Western-blot analyses, RT-qPCR. C.M. and K.L. performed the lipase and lipid analysis. C.M. performed the calorimetric and mouse activity analysis. O.L.B. and C.M analyzed the data. O.L.B. and S.W conceived and designed the experiments. O.L.B., Y.B., N.S. and S.W wrote the paper.

This study was supported by funding from the Région Auvergne to O. Le Bacquer. We thank Dr. Nahum Sonenberg (McGill University, Montréal, Canada) for providing with 4E-BP1/2 DKO mice. We thank Christophe Del'Homme, Julien Hermet and Medhi Djelloul from the Unité d'Expérimentation en Nutrition (INRA Clermont-Ferrand-Theix, France) for excellent assistance with animal care and for maintaining the mouse colonies.

The authors have declared no conflict of interest.

5 References

[1] Laplante, M., Sabatini, D. M., mTOR signaling in growth control and disease. *Cell* 2012, *149*, 274–293.

[2] Sonenberg, N., Hinnebusch, A. G., Regulation of translation initiation in eukaryotes: mechanisms and biological targets. *Cell* 2009, *136*, 731–745.

[3] Le Bacquer, O., Martineau, Y., Mamane, Y., When translation arises from its TORpor. *Med. Sci.* 2006, *22*, 514–518.

[4] Pause, A., Belsham, G. J., Gingras, A. C., Donze, O. et al., Insulin-dependent stimulation of protein synthesis by phosphorylation of a regulator of 5′-cap function. *Nature* 1994, *371*, 762–767.

[5] Poulin, F., Gingras, A. C., Olsen, H., Chevalier, S. et al., 4E-BP3, a new member of the eukaryotic initiation factor 4E-binding protein family. *J. Biol. Chem.* 1998, *273*, 14002–14007.

[6] Haghighat, A., Mader, S., Pause, A., Sonenberg, N., Repression of cap-dependent translation by 4E-binding protein 1: competition with p220 for binding to eukaryotic initiation factor-4E. *EMBO J.* 1995, *14*, 5701–5709.

[7] Raught, B., Gingras, A. C., Sonenberg, N., The target of rapamycin (TOR) proteins. *Proc. Natl. Acad. Sci. U. S. A.* 2001, *98*, 7037–7044.

[8] Gingras, A. C., Gygi, S. P., Raught, B., Polakiewicz, R. D. et al., Regulation of 4E-BP1 phosphorylation: a novel two-step mechanism. *Genes Dev.* 1999, *13*, 1422–1437.

[9] Gingras, A. C., Raught, B., Gygi, S. P., Niedzwiecka, A. et al., Hierarchical phosphorylation of the translation inhibitor 4E-BP1. *Genes Dev.* 2001, *15*, 2852–2864.

[10] Cornu, M., Albert, V., Hall, M. N., mTOR in aging, metabolism, and cancer. *Curr. Opin. Genet. Dev.* 2013, *23*, 53–62.

[11] Khamzina, L., Veilleux, A., Bergeron, S., Marette, A., Increased activation of the mammalian target of rapamycin pathway in liver and skeletal muscle of obese rats: possible involvement in obesity-linked insulin resistance. *Endocrinology* 2005, *146*, 1473–1481.

[12] Le Bacquer, O., Petroulakis, E., Paglialunga, S., Poulin, F. et al., Elevated sensitivity to diet-induced obesity and insulin resistance in mice lacking 4E-BP1 and 4E-BP2. *J. Clin. Invest.* 2007, *117*, 387–396.

[13] Um, S. H., Frigerio, F., Watanabe, M., Picard, F. et al., Absence of S6K1 protects against age- and diet-induced obesity while enhancing insulin sensitivity. *Nature* 2004, *431*, 200–205.

[14] Dungan, C. M., Li, J., Williamson, D. L., Caloric restriction normalizes obesity-induced alterations on regulators of skeletal muscle growth signaling. *Lipids* 2016, *51*, 905–912.

[15] Li, Z., Dungan, C. M., Carrier, B., Rideout, T. C. et al., Alpha-lipoic acid supplementation reduces mTORC1 signaling in

skeletal muscle from high fat fed, obese Zucker rats. *Lipids* 2014, *49*, 1193–1201.

[16] Shum, M., Bellmann, K., St-Pierre, P., Marette, A., Pharmacological inhibition of S6K1 increases glucose metabolism and Akt signalling in vitro and in diet-induced obese mice. *Diabetologia* 2016, *59*, 592–603.

[17] Drake, J. C., Alway, S. E., Hollander, J. M., Williamson, D. L., AICAR treatment for 14 days normalizes obesity-induced dysregulation of TORC1 signaling and translational capacity in fasted skeletal muscle. *Am. J. Physiol. Regul. Integr. Comp. Physiol.* 2010, *299*, R1546–1554.

[18] Polak, P., Cybulski, N., Feige, J. N., Auwerx, J. et al., Adipose-specific knockout of raptor results in lean mice with enhanced mitochondrial respiration. *Cell Metab.* 2008, *8*, 399–410.

[19] Tsukiyama-Kohara, K., Poulin, F., Kohara, M., DeMaria, C. T. et al., Adipose tissue reduction in mice lacking the translational inhibitor 4E-BP1. *Nat. Med.* 2001, *7*, 1128–1132.

[20] Tsai, S. Y., Rodriguez, A. A., Dastidar, S. G., Del Greco, E. et al., Increased 4E-BP1 expression protects against diet-induced obesity and insulin resistance in male mice. *Cell Rep.* 2016, *16*, 1903–1914.

[21] Tsai, S., Sitzmann, J. M., Dastidar, S. G., Rodriguez, A. A. et al., Muscle-specific 4E-BP1 signaling activation improves metabolic parameters during aging and obesity. *J. Clin. Invest.* 2015, *125*, 2952–2964.

[22] Tardif, N., Salles, J., Guillet, C., Tordjman, J. et al., Muscle ectopic fat deposition contributes to anabolic resistance in obese sarcopenic old rats through eIF2alpha activation. *Aging Cell* 2014, *13*, 1001–1011.

[23] Consitt, L. A., Bell, J. A., Houmard, J. A., Intramuscular lipid metabolism, insulin action, and obesity. *IUBMB Life* 2009, *61*, 47–55.

[24] Badin, P. M., Langin, D., Moro, C., Dynamics of skeletal muscle lipid pools. *Trends Endocrinol. Metab.* 2013, *24*, 607–615.

[25] Goodman, C. A., Mabrey, D. M., Frey, J. W., Miu, M. H. et al., Novel insights into the regulation of skeletal muscle protein synthesis as revealed by a new nonradioactive in vivo technique. *FASEB J* 2011, *25*, 1028–1039.

[26] Summers, S. A., Sphingolipids and insulin resistance: the five Ws. *Curr. Opin. Lipidol.* 2010, *21*, 128–135.

[27] Watt, M. J., Hoy, A. J., Lipid metabolism in skeletal muscle: generation of adaptive and maladaptive intracellular signals for cellular function. *Am. J. Physiol. Endocrinol. Metab.* 2012, *302*, E1315–1328.

[28] Zimmermann, R., Strauss, J. G., Haemmerle, G., Schoiswohl, G. et al., Fat mobilization in adipose tissue is promoted by adipose triglyceride lipase. *Science* 2004, *306*, 1383–1386.

[29] Takeuchi, K., Reue, K., Biochemistry, physiology, and genetics of GPAT, AGPAT, and lipin enzymes in triglyceride synthesis. *Am. J. Physiol. Endocrinol. Metab.* 2009, *296*, E1195–1209.

[30] Shi, Y., Cheng, D., Beyond triglyceride synthesis: the dynamic functional roles of MGAT and DGAT enzymes in energy metabolism. *Am. J. Physiol. Endocrinol. Metab.* 2009, *297*, E10–18.

[31] Dennis, M. D., Kimball, S. R., Jefferson, L. S., Mechanistic target of rapamycin complex 1 (mTORC1)-mediated phosphorylation is governed by competition between substrates for interaction with raptor. *J. Biol. Chem.* 2013, *288*, 10–19.

[32] Guridi, M., Tintignac, L. A., Lin, S., Kupr, B. et al., Activation of mTORC1 in skeletal muscle regulates whole-body metabolism through FGF21. *Sci. Signal.* 2015, *8*, ra113.

[33] Guridi, M., Kupr, B., Romanino, K., Lin, S. et al., Alterations to mTORC1 signaling in the skeletal muscle differentially affect whole-body metabolism. *Skelet. Muscle* 2016, *6*, 13.

[34] Singh, M., Shin, Y. K., Yang, X., Zehr, B. et al., 4E-BPs control fat storage by regulating the expression of Egr1 and ATGL. *J. Biol. Chem.* 2015, *290*, 17331–17338.

[35] Haemmerle, G., Zimmermann, R., Hayn, M., Theussl, C. et al., Hormone-sensitive lipase deficiency in mice causes diglyceride accumulation in adipose tissue, muscle, and testis. *J. Biol. Chem.* 2002, *277*, 4806–4815.

[36] Biolo, G., Wolfe, R. R., Insulin action on protein metabolism. *Baillieres Clin. Endocrinol. Metab.* 1993, *7*, 989–1005.

[37] Workeneh, B., Bajaj, M., The regulation of muscle protein turnover in diabetes. *Int. J. Biochem. Cell Biol.* 2013, *45*, 2239–2244.

[38] Guillet, C., Masgrau, A., Walrand, S., Boirie, Y., Impaired protein metabolism: interlinks between obesity, insulin resistance and inflammation. *Obes. Rev.* 2012, *13*(Suppl 2), 51–57.

[39] Anderson, S. R., Gilge, D. A., Steiber, A. L., Previs, S. F., Diet-induced obesity alters protein synthesis: tissue-specific effects in fasted versus fed mice. *Metab. Clin. Exp.* 2008, *57*, 347–354.

[40] Guillet, C., Prod'homme, M., Balage, M., Gachon, P. et al., Impaired anabolic response of muscle protein synthesis is associated with S6K1 dysregulation in elderly humans. *FASEB J.* 2004, *18*, 1586–1587.

[41] Webster, J. D., Hesp, R., Garrow, J. S., The composition of excess weight in obese women estimated by body density, total body water and total body potassium. *Hum. Nutr. Clin. Nutr.* 1984, *38*, 299–306.

[42] Kemp, J. G., Blazev, R., Stephenson, D. G., Stephenson, G. M., Morphological and biochemical alterations of skeletal muscles from the genetically obese (ob/ob) mouse. *Int. J. Obes.* 2009, *33*, 831–841.

[43] Durschlag, R. P., Layman, D. K., Skeletal muscle growth in lean and obese Zucker rats. *Growth* 1983, *47*, 282–291.

[44] Thibault, R., Chanseaume, S., Azarnoush, K., Guillet, C. et al., Mitochondrial protein synthesis is increased in oxidative skeletal muscles of rats with cardiac cachexia. *Nutr. Res.* 2014, *34*, 250–257.

[45] Adechian, S., Giardina, S., Remond, D., Papet, I. et al., Excessive energy intake does not modify fed-state tissue protein synthesis rates in adult rats. *Obesity* 2009, *17*, 1348–1355.

[46] Masgrau, A., Mishellany-Dutour, A., Murakami, H., Beaufrere, A. M. et al., Time-course changes of muscle protein synthesis associated with obesity-induced lipotoxicity. *J. Physiol.* 2012, *590*, 5199–5210.

[47] Banko, J. L., Poulin, F., Hou, L., DeMaria, C. T. et al., The translation repressor 4E-BP2 is critical for eIF4F complex formation, synaptic plasticity, and memory in the hippocampus. *J. Neurosci.* 2005, *25*, 9581–9590.

[48] Banko, J. L., Merhav, M., Stern, E., Sonenberg, N. et al., Behavioral alterations in mice lacking the translation repressor 4E-BP2. *Neurobiol. Learn. Mem.* 2007, *87*, 248–256.

[49] Risson, V., Mazelin, L., Roceri, M., Sanchez, H. et al., Muscle inactivation of mTOR causes metabolic and dystrophin defects leading to severe myopathy. *J. Cell Biol.* 2009, *187*, 859–874.

[50] Bentzinger, C. F., Lin, S., Romanino, K., Castets, P. et al., Differential response of skeletal muscles to mTORC1 signaling during atrophy and hypertrophy. *Skelet. Muscle* 2013, *3*, 6.

[51] Ohanna, M., Sobering, A. K., Lapointe, T., Lorenzo, L. et al., Atrophy of S6K1(-/-) skeletal muscle cells reveals distinct mTOR effectors for cell cycle and size control. *Nat. Cell Biol.* 2005, *7*, 286–294.

[52] Goodman, C. A., Miu, M. H., Frey, J. W., Mabrey, D. M. et al., A phosphatidylinositol 3-kinase/protein kinase B-independent activation of mammalian target of rapamycin signaling is sufficient to induce skeletal muscle hypertrophy. *Mol. Biol. Cell* 2010, *21*, 3258–3268.

[53] Steiner, J. L., Pruznak, A. M., Deiter, G., Navaratnarajah, M. et al., Disruption of genes encoding eIF4E binding proteins-1 and -2 does not alter basal or sepsis-induced changes in skeletal muscle protein synthesis in male or female mice. *PloS One* 2014, *9*, e99582.

[54] Signer, R. A., Qi, L., Zhao, Z., Thompson, D. et al., The rate of protein synthesis in hematopoietic stem cells is limited partly by 4E-BPs. *Genes Dev.* 2016, *30*, 1698–1703.

[55] Harrington, L. S., Findlay, G. M., Lamb, R. F., Restraining PI3K: mTOR signalling goes back to the membrane. *Trends Biochem. Sci.* 2005, *30*, 35–42.

[56] Haruta, T., Uno, T., Kawahara, J., Takano, A. et al., A rapamycin-sensitive pathway down-regulates insulin signaling via phosphorylation and proteasomal degradation of insulin receptor substrate-1. *Mol. Endocrinol.* 2000, *14*, 783–794.

[57] Zhang, Y., Nicholatos, J., Dreier, J. R., Ricoult, S. J. et al., Coordinated regulation of protein synthesis and degradation by mTORC1. *Nature* 2014, *513*, 440–443.

